Estimation of maize evapotranspiration using extreme learning machine and generalized regression neural network on the China Loess Plateau

Yu Feng, Daozhi Gong, Xurong Mei and Ningbo Cui

ABSTRACT

Accurately estimating crop evapotranspiration (*ET*) is essential for agricultural water management in arid and semiarid croplands. This study developed extreme learning machine (ELM) and generalized regression neural network (GRNN) models for maize *ET* estimation on the China Loess Plateau. Maize *ET*, meteorological variables, leaf area index (*LAI*), and plant height (h_c) were continuously measured during maize growing seasons of 2011–2013. The meteorological data and crop data including *LAI* and h_c from 2011 to 2012 were used to train the ELM and GRNN using two different input combinations. The performances of ELM and GRNN were compared with the modified dual crop coefficient (K_c) approach in 2013. Results indicated that ELM1 and GRNN1 using meteorological and crop data as inputs estimated maize *ET* accurately, with root mean square error (RMSE) of 0.221 mm/d, mean absolute error (MAE) of 0.203 mm/d, and NS of 0.981 for ELM1, RMSE of 0.225 mm/d, MAE of 0.211 mm/d, and NS of 0.981 for GRNN1, respectively, which confirmed better performances than the modified dual K_c model. Performances of ELM2 and GRNN2 using only meteorological data as input were poorer than those of ELM1, GRNN1, and modified dual K_c approach, but its estimation of maize *ET* was acceptable when only meteorological data were available.

Key words | evapotranspiration, extreme learning machine, generalized regression neural network, maize, modified dual crop coefficient approach

Yu Feng
Daozhi Gong (corresponding author)
Xurong Mei
State Engineering Laboratory of Efficient Water Use of Crops and Disaster Loss Mitigation/MOA Key Laboratory for Dryland Agriculture,
Institute of Environment and Sustainable Development in Agriculture, Chinese Academy of Agriculture Sciences,
Beijing,
China
E-mail: *gongdaozhi@caas.cn*

Ningbo Cui
State Key Laboratory of Hydraulics and Mountain River Engineering,
College of Water Resource and Hydropower, Sichuan University,
Chengdu,
China

INTRODUCTION

Population growth and increasing consumption of calorie- and meat-intensive diets are expected to roughly double human food demand by 2050 (Mueller *et al.* 2012). To meet this increasing food demand in the coming decades, new practices for agricultural water management must be developed, especially in arid and semiarid regions, to boost crop production per amount of water use, i.e., crop water use efficiency (WUE). As the only term that appears in both water balance and surface energy balance equations (Xu & Singh 2005), evapotranspiration (*ET*) is not only the basis of a deep understanding of ecological and hydrological processes, but also an important indicator to evaluate WUE in agriculture. About half the lands on Earth are short of water (Newman *et al.* 2006), and more than 90% of water used in agriculture is lost by *ET* (Rana & Katerji 2000; Ding *et al.* 2013). Therefore, accurate estimation of *ET* is of importance to regional agricultural water management aiming at water saving and an increase of WUE (Zhang *et al.* 2013).

In the past decades, numerous methods, which can be grouped into single-layer (e.g., Penman–Monteith), two-layer (e.g., Shuttleworth–Wallace) and multi-layer (e.g., Clummping) models (Monteith 1965; Shuttleworth & Wallace 1985; Brenner & Incoll 1997), have been proposed for *ET* estimation since direct measurement of *ET* is difficult, costly, and not available in many regions (Allen *et al.* 1998; Ding *et al.* 2013). The main limitation of these methods developed on a physical basis, however, is their required input data cannot be easily measured, such as aerodynamic

doi: 10.2166/nh.2016.099

resistance and surface resistance (Allen 2000; Ding *et al.* 2013). To overcome this deficiency, the indirect FAO-56 dual crop coefficient approach was proposed by Allen *et al.* (1998), which was the product of reference evapotranspiration (ET_0) and crop coefficient (K_c). ET_0 is the evapotranspiration rate of the reference crop with an assumed crop height of 0.12 m, a fixed surface resistance of 70 s/m, and an albedo of 0.23, while K_c, the ratio of *ET* and ET_0, represents the effects of characteristics that distinguish the specific field crops from the reference crop. Compared with the single K_c method, the dual K_c approach makes it possible to better assess the impacts of soil wetting by rain or irrigation, as well as the impacts of keeping part of the soil dry or using mulches for controlling soil evaporation (Zhang *et al.* 2013), and has been widely applied for *ET* estimation due to the simplicity and good performances of the approach (Allen 2000; Rousseaux *et al.* 2009; Liu & Luo 2010; Ferreira *et al.* 2012; Zhao *et al.* 2015). Although good performances of this approach have been widely reported, the straightforward adoption of generalized crop coefficients recommended by FAO-56 can lead to errors in the estimation of *ET* since the dividing of crop growth period and associated crop coefficients are closely related to local climate and crop conditions (Katerji & Rana 2006; Poblete-Echeverría & Ortega-Farias 2013; Zhao *et al.* 2015). Thus, a modification of the dual K_c approach is needed when applying the method for *ET* estimation.

In recent years, artificial intelligence (AI) has been successfully implemented in ET_0 estimation. The application of AI in ET_0 modeling was first investigated after 2000 by Kumar *et al.* (2002), who estimated ET_0 using an artificial neural network (ANN). Since then, efforts towards the estimation of ET_0 using ANN models have been performed (Trajkovic *et al.* 2003; Kisi 2006; Kim & Kim 2008; Landeras *et al.* 2008; Traore *et al.* 2010; Martí *et al.* 2011a). More recently, many studies have proposed some new AI approaches for ET_0 estimation: Tabari *et al.* (2012) investigated the performances of support vector machines, adaptive neuro-fuzzy inference system for ET_0 estimation in a semi-arid highland environment in Iran; Shiri *et al.* (2011, 2012) applied a genetic programming approach for ET_0 and evaporation modeling; Kisi *et al.* (2012) developed generalized neurofuzzy-based evaporation models in Arizona, USA; Pour Ali Baba *et al.* (2013) estimated ET_0 using adaptive neuro-fuzzy inference system and ANN for two weather stations in South Korea; Kisi (2013) investigated the applicability of Mamdani and Sugeno fuzzy genetic approaches in modeling ET_0 in Turkey; Shiri *et al.* (2013) and Martí *et al.* (2015) used gene expression programming for ET_0 estimation; Kisi (2016) investigated the ability of least square support vector regression, multivariate adaptive regression splines and M5 Model Tree in modeling ET_0 in Turkey; Abdullah *et al.* (2015) and Feng *et al.* (2016) examined the capability of extreme learning machine (ELM) for ET_0 estimation in Iraq and Southwest China, respectively. All these studies confirmed good performances of AI approaches for ET_0 estimation worldwide. Differently to ET_0, which is from a reference crop and only affected by meteorological variables, *ET* for a specific crop is more complicated and affected not only by meteorological variables but also soil properties, crop characteristics, and agronomy management. To the best knowledge of the authors, there are no former studies evaluating the performances of AI approaches for rainfed maize *ET* estimation considering experimental data as targets.

This study applied two AI approaches, i.e., ELM and generalized regression neural network (GRNN), for maize *ET* estimation using meteorological and crop data on the China Loess Plateau. The performances of ELM and GRNN were assessed against the modified dual K_c approach for evaluating the newly proposed models considering measured maize *ET* data from eddy covariance systems in a rainfed cropland as benchmark.

MATERIALS AND METHODS

Study site

The study was carried out in a rainfed spring maize field at the Experimental Station of Dryland Agriculture and Environment (ESDAE), Ministry of Agriculture, P. R. China, which is located in Shouyang, Shanxi Province, northern P. R. China (37 °45′58″N,113 °12′9″E, 1,202 m Alt.) during three maize growing seasons (from May 1 to September 28, 2011, May 3 to September 22, 2012, and April 28 to September 25, 2013). The experimental station has a typical continental temperate climate with a mean daily temperature of 7.4 °C, mean annual precipitation of 481 mm and mean

annual frost-free days of 140 days. Mean annual precipitation during the growing season of spring maize is about 330 mm. The soil at the experimental station is classified as a cinnamon soil with light clay loam texture and an average bulk density of 1.34 g/cm^3. Average volumetric soil water content at field capacity and wilting point were 36.0% and 12.0% to a depth of 1.0 m, respectively. Groundwater is about 150 m below ground surface (Gong *et al.* 2015).

The maize crop, variety Jingdan-951, was sown in north–south rows with the distance between rows equal to 50 cm and the space between two plants within rows of 30 cm. The maize sowing rate was 66,667 seeds per ha for 3 years. The area of the experiment plots is about 3.0 ha, of which length and width is 200 m and 150 m, respectively, which meets the minimum fetch requirement of eddy covariance system installation (Gong *et al.* 2015).

Measurements

Meteorological data

Half-hourly meteorological variables were obtained by an automatic weather station (Campbell Scientific Inc., Logan, UT, USA) nearby the experimental plots (Gong *et al.* 2015). Solar radiation (R_s) was measured with a Silicon Pyranometer (LI200X, LI-COR, Inc., Lincoln, NE, USA) and precipitation (P) was registered with a pluviometer (RGB1, Campbell Scientific Inc.). Wind speed (u_2) and its direction (w) were measured using a cup anemometer and a wind vane (03002-L, R. M. Young Inc., Traverse, MI, USA), respectively. Air temperature (T) and relative humidity (RH) were measured using a Vaisala probe (HMP45C, Vaisala Inc., Tucson, AZ, USA). All variables were monitored at 2 m above the surface and recorded in a datalogger (CR10RX, Campbell Scientific Inc.).

Eddy covariance system and evapotranspiration measurements

In the center of the experimental plot, latent (LE) and sensible heat (H) fluxes were measured by an open-path eddy covariance system mounted on a tower, which consisted of an open-path infrared gas analyzer (LI-COR Inc., model LI-7500) and a three-dimensional supersonic anemometer (Campbell Scientific Inc., model CSAT3). A temperature and humidity sensor (Campbell Scientific Inc., model HMP45C), a four-way net radiometer (Kipp & Zonen Inc., Delftechpark, The Netherlands, model CNR1), and self-calibrating heat flux sensors (Campbell Scientific Inc., model HFP01) were also used. The sensor height was adjusted to keep the relative height of 0.5 m between sensors and maize canopy constant at interval of 5–7 days. Specific time length depended on the increments of canopy height. The observation site had a wide fetch of at least 50 m in all directions, which allowed us to neglect heat advection in the maize field (Gong *et al.* 2015). All of the measured meteorological and fluxes data were averaged at daily timescale in the present study.

Leaf area index and plant height measurements

Five maize plants were randomly selected to measure plants height (h_c), leaf length, and width at internal of 1 or 2 weeks during the maize growing season. Specific time length depended on maize growth stages and leaf growth rates. Leaf area index (LAI) was calculated by summing products of lamina length and maximum width of each leaf and then multiplying by an empirical coefficient of 0.74, and then dividing by area per plant (30 cm × 50 cm) (Li *et al.* 2008; Gong *et al.* 2015):

$$LAI = 0.74 \times \frac{\sum_{i=1}^{n} L_i \times W_i}{D_{row} \times S_{plant}} \quad (1)$$

where LAI is leaf area index (m^2/m^2); L_i and W_i is the length and width of the i-th leaf, respectively; D_{row} and S_{plant} stand for the distance between the two rows and the space between the plants in the row, respectively.

The modified dual K_c approach for ET estimation

Reference evapotranspiration

Daily reference evapotranspiration (ET_0) was estimated using the FAO-56 Penman–Monteith equation (Allen *et al.* 1998; Feng *et al.* 2014):

$$ET_0 = \frac{0.408\Delta(R_n - G) + \gamma \frac{900}{T_{mean} + 273} u_2 (e_s - e_a)}{\Delta + \gamma(1 + 0.34u_2)} \quad (2)$$

where ET_0 is reference evapotranspiration (mm/d); R_n is net radiation (MJ/m^2 d); G is soil heat flux density (MJ/m^2 d); T_{mean} is mean air temperature (°C); e_s is saturation vapor pressure, kPa; e_a is actual vapor pressure, kPa; Δ is slope of the saturation vapor pressure function (kPa/°C); γ is psychometric constant (kPa/°C); and u_2 is wind speed at 2 m height (m/s).

Maize ET

Actual maize ET was calculated by multiplying ET_0 and K_c (Allen *et al.* 1998):

$$ET = ET_0 \times K_c \tag{3}$$

According to the dual K_c approach, K_c can be split into two parameters, which are K_e and K_{cb}. Thus, Equation (3) can be rewritten as:

$$ET = (K_s K_{cb} + K_e)ET_0 = K_s K_{cb} ET_0 + K_e ET_0 \tag{4}$$

where ET is crop evapotranspiration (mm/d); K_{cb} is basal crop coefficient; K_e is soil evaporation coefficient; K_s is water stress coefficient. Thus, $K_s K_{cb} ET_0$ represents crop transpiration while $K_e ET_0$ represents soil evaporation.

(1) Calculation of K_{cb}:

According to FAO-56, the original K_{cb} is calculated as (Allen *et al.* 1998):

$$K_{cb,o} = K_{cb(Tab)} + [0.04(u_2 - 2) - 0.004(RH_{min} - 45)] \times \left(\frac{h_c}{3}\right)^{0.3} \tag{5}$$

where $K_{cb,o}$ is the original basal crop coefficient obtained; $K_{cb(Tab)}$ is basal crop coefficient value taken from FAO-56 recommendation; u_2 is wind speed at 2 m height (m/s); RH_{min} is minimum daily relative humidity (%); and h_c is crop height (m).

This study applied canopy cover coefficient (K_{cc}) to accurately calculate daily actual K_{cb} (Ding *et al.* 2013):

$$K_{cb} = K_{c,min} + K_{cc}(K_{cb,full} - K_{c,min}) \tag{6}$$

where $K_{c,min}$ is the minimum basal crop coefficient for bare soil; $K_{cb,full}$ is basal crop coefficient when crop has nearly full ground cover. $K_{cb,full}$ can be calculated following the method of Allen *et al.* (1998):

$$K_{cb,full} = \min(1.0 + 0.1h_c, K_{max}) + [0.04(u_2 - 2) - 0.004(RH_{min} - 45)]\left(\frac{h_c}{3}\right)^{0.3} \tag{7}$$

K_{cc} was then calculated by the ratio of radiation intercepted by crop canopy:

$$K_{cc} = 1 - e^{-\kappa \cdot \mathrm{LAI}} \tag{8}$$

where κ is the coefficient for radiation extinguish and LAI is leaf area index.

(2) Calculation of K_e:

K_e is calculated by estimating energy availability and soil moisture regimes at the soil surface through the original FAO-56 procedure:

$$K_e = K_r(K_{c,max} - K_{cb}) \le f_{ew} K_{c,max} \tag{9}$$

where K_e is the soil evaporation coefficient; $K_{c,max}$ is the maximum value of K_c following rain or irrigation; K_r is evaporation reduction coefficient; f_{ew} is the fraction of the soil that is both exposed to solar radiation and wetted (0.01–1.0). Evaporation is restricted by the energy available at the exposed soil fraction, i.e., K_e could not exceed few $K_{c,max}$.

$K_{c,max}$ is adjusted for crop height and climate:

$$K_{c,max} = \max\left(\left\{1.2 + [0.04(u_2 - 2) - 0.004(RH_{min} - 45)]\left(\frac{h_c}{3}\right)^{0.3}\right\}, \{K_{cb} + 0.05\}\right) \tag{10}$$

$$f_{ew} = \min(1 - f_c, f_w) \tag{11}$$

$$K_r = \frac{TEW - D_{e,i-1}}{TEW - REW} \tag{12}$$

where f_c is the approximate fraction of soil surface that is exposed; f_w is the average fraction of soil surface wetted by irrigation or precipitation; $D_{e,i-1}$ is cumulative depth of evaporation from the soil surface layer at the end of day $i-1$ (mm); TEW is total evaporable water (mm); REW is readily

evaporable water (mm). When $D_{e,i-1} \leq REW$, $K_r = 1.0$.

$$TEW = 1000(\theta_{FC} - 0.5\theta_{WP})Z_e \quad (13)$$

where θ_{FC} and θ_{WP} are soil water contents at field capacity and wilting point, respectively (m^3/m^3). Z_e is depth of the topsoil layer.

f_c was determined by LAI:

$$f_c = 1.005[1 - \exp(-0.6\mathrm{LAI})]^{1.2} \quad (14)$$

D_e calculation requires a daily water budget for the exposed and wetted surface.

$$D_{e,i} = D_{e,i-1} - (P_i - RO_i) + \frac{E_i}{f_{ew}} + T_{ew,i} + DP_{e,i} \quad (15)$$

where $D_{e,i}$ and $D_{e,i-1}$ are cumulative depth of evaporation of the topsoil at the end of day i and $i-1$ (mm); P_i is precipitation on day i (mm); RO_i is runoff from the soil surface on day i (mm); E_i is evaporation on day i (mm); $T_{ew,i}$ is depth of transpiration of the soil surface layer on day i (mm), $T_{ew,i} = 0$ for row crops as recommended in Allen *et al.* (1998); $DP_{e,i}$ is deep percolation loss from the topsoil layer on day i if soil water content exceeds field capacity (mm).

(3) Calculation of water stress coefficient:

$$K_s = \begin{cases} 1 & D_r \leq RAW \\ \dfrac{TAW - D_r}{TAW - RAW} & D_r > RAW \end{cases} \quad (16)$$

where $D_{r,i-1}$ is root zone depletion at the end of day $i-1$ (mm); TAW is total available water in the root zone (mm); RAW is the readily available soil water in the root zone (mm). When $D_{r,i-1} < RAW$, $K_s = 1.0$.

$$TAW = 1000(\theta_{FC} - \theta_{WP})Z_r \quad (17)$$

where Z_r is the rooting depth (m).

AI models for *ET* estimation

Extreme learning machine

The ELM was first proposed by Huang *et al.* (2006). Its learning speed can be thousands of times faster than traditional feedforward neural network (FFNN) learning algorithms such as back-propagation algorithm while obtaining better generalization performance. For traditional FFNN, all the parameters need to be tuned and thus there exists a dependency between different layers of parameters (weights and biases) (Huang *et al.* 2006). The advantage of ELM is that the hidden layer does not need to be tuned and the learning speed is faster than traditional FFNN, in addition to better generalization performance (Abdullah *et al.* 2015). The ELM has successfully been applied for function approximation in hydrology, e.g., daily streamflow forecasting (Rasouli *et al.* 2012), rainfall–runoff modeling (Taormina & Chau 2015). Recently, Abdullah *et al.* (2015) and Feng *et al.* (2016) found ELM had very good generalization performances for ET_0 estimation. In this study, we applied ELM for maize *ET* estimation, and different combinations of meteorological and crop were selected as input to train ELM. Figure 1 presents the structure of the ELM model, which consists of input layer (input variables), hidden layer (neurons), and output layer (*ET*). Different hidden nodes were used to estimate maize *ET* (e.g., 10, 20, 30, … , 200), and we found that with the increase of hidden nodes, the error of the ELM model reduced significantly and this reduction was not so significant after hidden nodes exceeded 100. Thus, 100 hidden nodes proved efficient to estimate maize *ET*. Further details about ELM may be found in Huang *et al.* (2006), Abdullah *et al.* (2015), and Feng *et al.* (2016).

Generalized regression neural network

The GRNN was first proposed by Specht (1991) and is a radial basis function network. GRNN approximates any arbitrary function between input and output vectors, drawing the function estimate directly from training data. Although it is similar to the common FFNN, its operation is fundamentally different

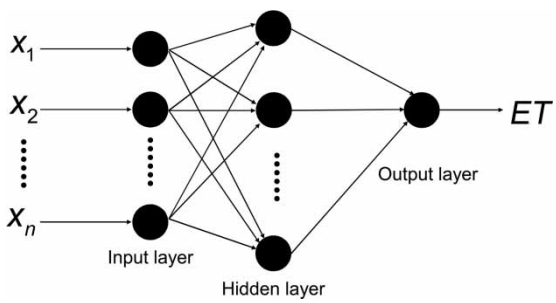

Figure 1 | The ELM structure.

in that it is based on nonlinear regression theory for function estimation. The training set consists of values of inputs x and produces the estimated value of y, which minimizes the squared error (Kisi 2006, 2008). The GRNN structure is presented in Figure 2. As shown in Figure 2, the GRNN consists of four layers, including the input layer (input variables), pattern layer, summation layer, and output layer (ET). The spread constants for the GRNN model are determined by using circuit training. Further details about GRNN for ET estimation can be found in Kisi (2006, 2008) and Ladlani *et al.* (2012). MATLAB software (R2015b) is utilized to implement ELM and GRNN for daily maize ET estimation.

Model training and assessment

Two different input combinations were selected to train the GRNN and ELM models. One considered meteorological and crop data as input, the same input data as the modified dual K_c approach, and the other combination considered meteorological data as input to evaluate the capabilities of the ELM and GRNN when only meteorological data are available. Table 1 presents a summary of the input combinations for each model. ELM1 and GRNN1 were fed with meteorological (maximum, minimum, and mean air temperature, maximum, minimum, and mean relative humidity, solar radiation, and wind speed at 2 m height) and crop data (leaf area index and plant height). ELM2 and GRNN2 were fed only with meteorological data since the crop data are not commonly available.

Although k-fold assessment is recommended for assessing the performances of AI models (Martí *et al.* 2011b, 2015; Shiri *et al.* 2014a, 2014b, 2015), a simple data set assignment was considered for this study. The k-fold assessment would have involved computational costs that could not be assumed. The considered assessment procedure is a very common practice for AI models' assessment (Shiri *et al.* 2014c). The data of 2011 and 2012 were used to train the ELM and GRNN models, and data of 2013 were applied to assess the performances of the models. Thus, 293 patterns were available for training, while 150 patterns were used for testing.

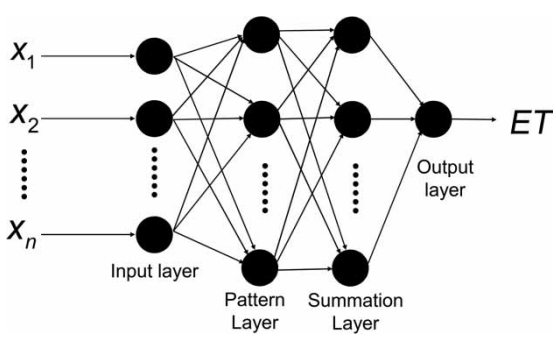

Figure 2 | The GRNN structure.

Table 1 | Summary of input combinations for each AI model

	Meteorological data				Crop data	
Model	***T***	***RH***	R_s	u_2	***LAI***	h_c
ELM1	√	√	√	√	√	√
GRNN1	√	√	√	√	√	√
ELM2	√	√	√	√		
GRNN2	√	√	√	√		

T is air temperature, including maximum, minimum, and mean air temperature; RH is relative humidity, including maximum, minimum, and mean relative humidity; R_s is solar radiation; u_2 is wind speed at 2 m height; LAI is leaf area index; h_c is plant height.

Performance evaluation

Root mean square error (RMSE), mean absolute error (MAE), and Nash–Sutcliffe coefficient (NS) were used to evaluate performances of the models:

$$RMSE = \sqrt{\frac{1}{n}\sum_{i=1}^{n}(ET_i^E - ET_i^M)} \tag{18}$$

$$MAE = \frac{\sum_{i=1}^{n}\left|ET_i^E - ET_i^M\right|}{n} \tag{19}$$

$$NS = 1 - \frac{\sum_{i=1}^{n}(ET_i^E - ET_i^M)^2}{\sum_{i=1}^{n}(ET_i^M - ET_{mean})^2} \tag{20}$$

where ET_i^M and ET_i^E are ET values at the i-th step obtained by measurement and estimation, respectively; n is the number of the time steps; ET_{mean} is the mean value of the measured ET values; RMSE and MAE are both in mm/d, taking on value from 0 (perfect fit) to ∞ (the worst fit); NS

is dimensionless, taking on value from 1 (perfect fit) to $-\infty$ (the worst fit).

RESULTS AND DISCUSSION

Variations of meteorological and crop variables

Figure 3 presents seasonal variations of meteorological variables during maize growing seasons of 2011–2013. Daily air temperature, including maximum, minimum, and mean air temperature, increased in initial and development stage, but decreased gradually in the mid and late stage, with average maximum, minimum, and mean air temperature of 23.5, 12.5, and 17.4 °C for 2011, 23.8, 13.5, 18.2 °C for 2012 and 25.2, 13.5, and 18.4 °C for 2013, respectively. Compared with minimum and mean relative humility, maximum relative humility had quite a different change pattern. It was lower at the initial and late stage, and maintained stable values above 90% due to heavier rainfall in the mid stage for 3 years, with average maximum, minimum, and mean relative humidity of 83.5%, 42.0%, and 66.9% for 2011, 84.5%, 42.8%, 67.7% for 2012 and 83.3%, 41.2%, and 66.5% for 2013, respectively. Solar radiation fluctuated significantly during the growing season for 3 years, and lower values can be observed in the initial and late stage with greater values in the development and mid stage, with average solar radiation of 18.6, 15.9, and 18.2 MJ/m^2 d for 3 years, respectively. An obvious declining trend of wind speed from initial to late stage could be found, with an average wind speed of 2.0, 2.0, and 1.8 m/s for 3 years, respectively. ET_0 increased in the initial stage and then decreased gradually to the late stage, with average ET_0 of 3.9, 3.9, and 4.2 mm/d. Precipitation fluctuated significantly during the growing season for 3 years, and total precipitation of 2011 was lower than that of 2013 and greater than that of 2012, with total precipitation of 496, 417, and 515 mm for 3 years, respectively.

Figure 4 presents seasonal variations of LAI and h_c for 3 years. LAI increased significantly after the initial stage, and reached a maximum in mid stage while decreasing in the late stage for all 3 years. Greater LAI can be observed in 2012, and it was about 2 weeks earlier than that of 2013 and 3 weeks earlier than that of 2011 when LAI reached the maximum, with LAI ranges of 0–3.64 m^2/m^2 for 2011, 0–4.52 m^2/m^2 for 2012, and 0–3.97 m^2/m^2 for 2013, respectively. Similarly, significant increases can be observed after the initial stage, and reached a maximum in mid stage. Greater h_c can be observed in 2012, with h_c ranges of 0–2.75 m for 2011, 0–2.98 m for 2012, and 0–2.97 m for 2013, respectively. Greater LAI and h_c in 2012 may be attributed to greater soil temperature and soil water content in 2012.

Energy balance closure of the eddy covariance system

The relationships between available energy (R_n-G) and turbulent fluxes ($LE + H$) at interval of 30 minutes for 3 years are presented in Figure 5. It is seen that the slopes of the linear regression varied from 0.78 to 0.92, with average energy balance closure of 0.86, which is within common results found in the literature for eddy covariance systems (Li *et al.* 2005; Allen *et al.* 2011). In accordance with the findings of other studies (Wilson *et al.* 2002; Wolf *et al.* 2008; Allen *et al.* 2011; Zhang *et al.* 2013), imbalance of the eddy covariance system in the experimental site was found, which may be attributed to the underestimation of ET (Wolf *et al.* 2008).

Parameters of dual K_c approach

Table 2 presents parameters of dual K_c approach for maize ET estimation in 2013. Z_e was 0.1 m in this study, recommended by FAO-56 (Allen *et al.* 1998). Measured maximum h_c and LAI were 2.97 m and 3.95 m^2/m^2, respectively. REW, TEW, and TAW were calibrated using soil property data, with values of 7, 23, and 181 mm, respectively. Greater TEW and TAW may be due to the fact that the soil in the experimental site was sandy loam, leading to a greater soil water content at field capacity (36.2%). According to Allen & Pereira (2009) and Ding *et al.* (2013), accurate estimation of canopy cover coefficient could be achieved when κ was 0.7.

Figure 6 presents seasonal variation of crop coefficient in 2013. The crop coefficient increased in the initial and development stage, and reached maximum in the mid stage, then decreased gradually in the late stage, with crop coefficient ranges of 0.06–0.26 in the initial stage, 0.15–0.82 in the development stage, 0.67–1.43 in the mid stage, and 0.54–1.22 in the late stage.

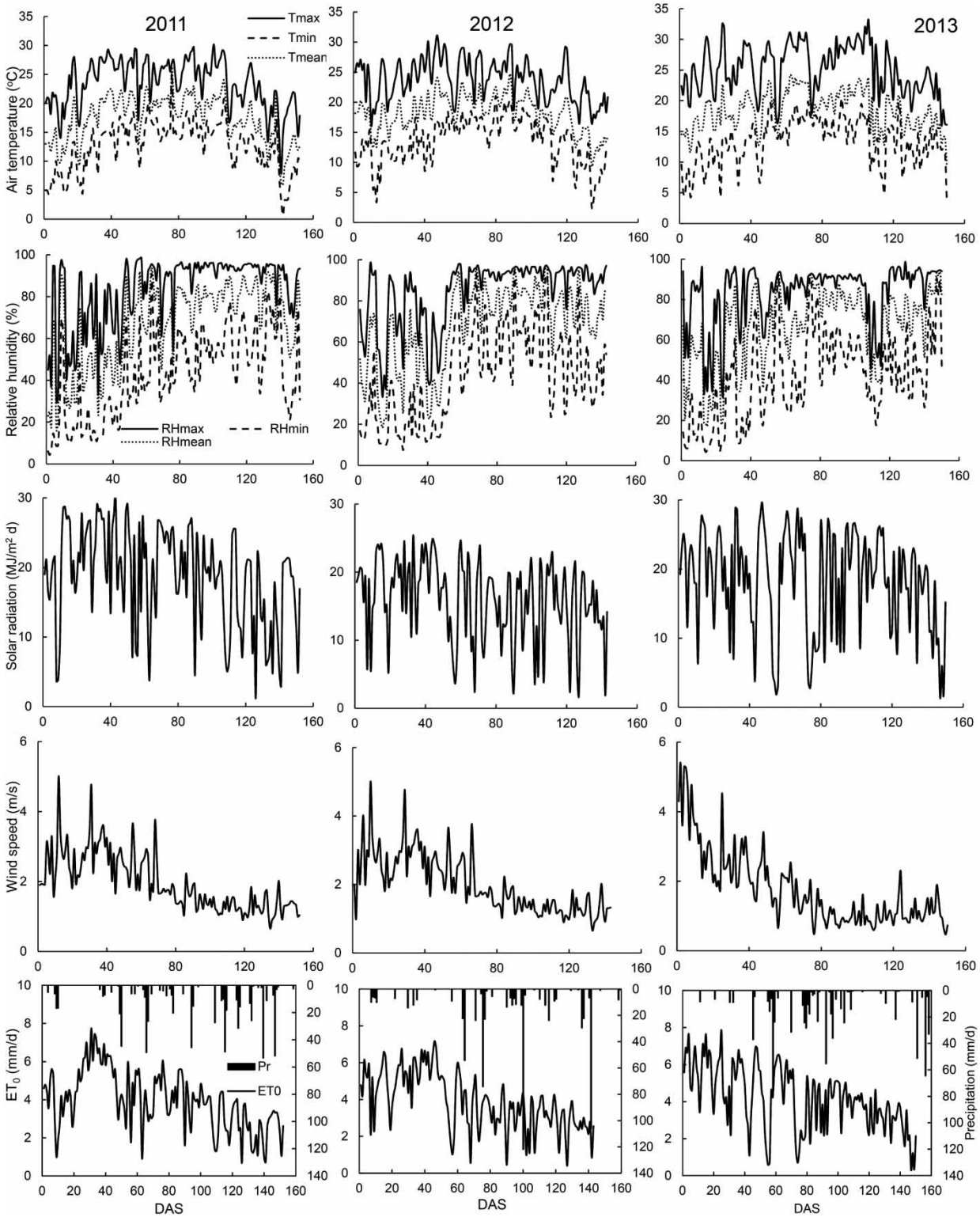

Figure 3 | Seasonal variations of meteorological variables during maize growing seasons of 2011–2013.

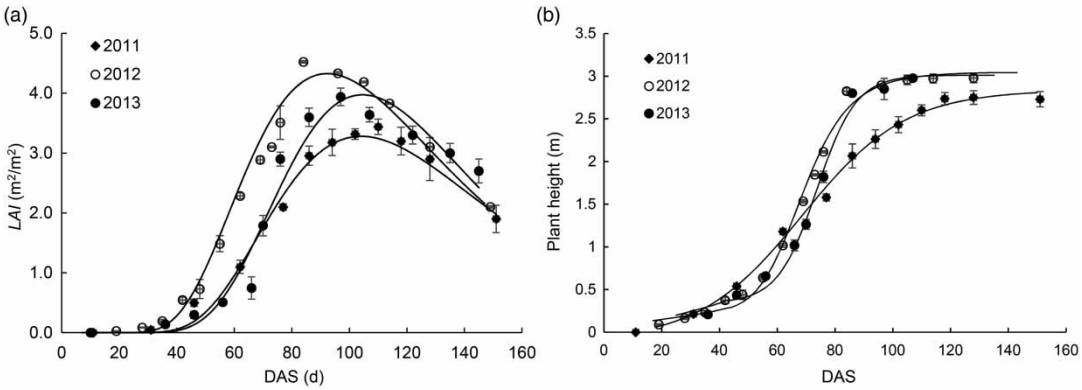

Figure 4 | Seasonal variations of leaf area index and plant height during maize growing seasons of 2011–2013.

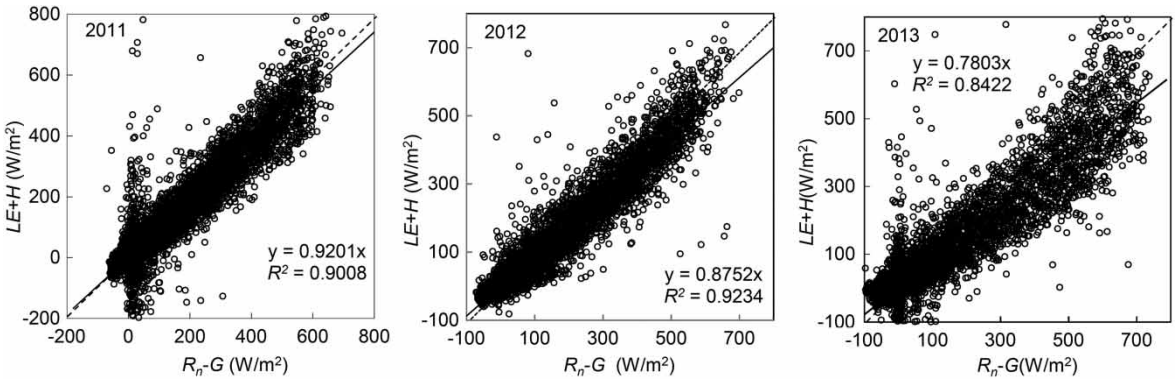

Figure 5 | Relationships between R_n-G and $LE + H$ at intervals of 30 minutes for 3 years.

Comparison of AI and dual K_c approaches

The comparison of the *ET* values estimated by the ELM, GRNN, and FAO-56 dual K_c models is shown in Figure 7, in the form of line graphs and scatter plots. It is seen from the line graphs and scatter plots that *ET* values estimated by the ELM1 model closely followed the measured *ET* values, and the slope of linear regression between estimated and measured *ET* was 0.974, with R^2 of 0.998; *ET* values estimated by the GRNN1 model closely followed the measured *ET* values too, and the slope of linear

Table 2 | Parameters of dual K_c approach for maize *ET* estimation in 2013

Parameters	Values	Units	Source
Z_e	0.1	m	Allen *et al.* (1998)
Maximum h_c	2.97	m	Measured
Maximum *LAI*	3.95	m^2/m^2	Measured
REW	7	mm	Calibrated
TEW	23	mm	Calibrated
TAW	181	mm	Calibrated
κ	0.7	–	Ding *et al.* (2013)

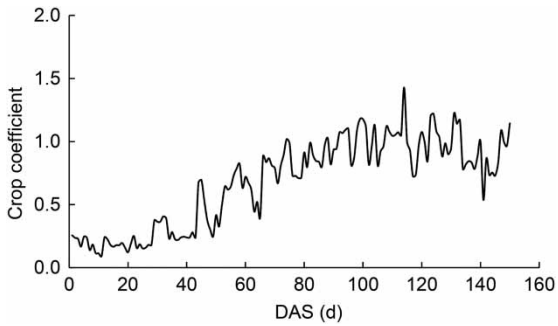

Figure 6 | Seasonal variation of crop coefficient during maize growing season of 2013.

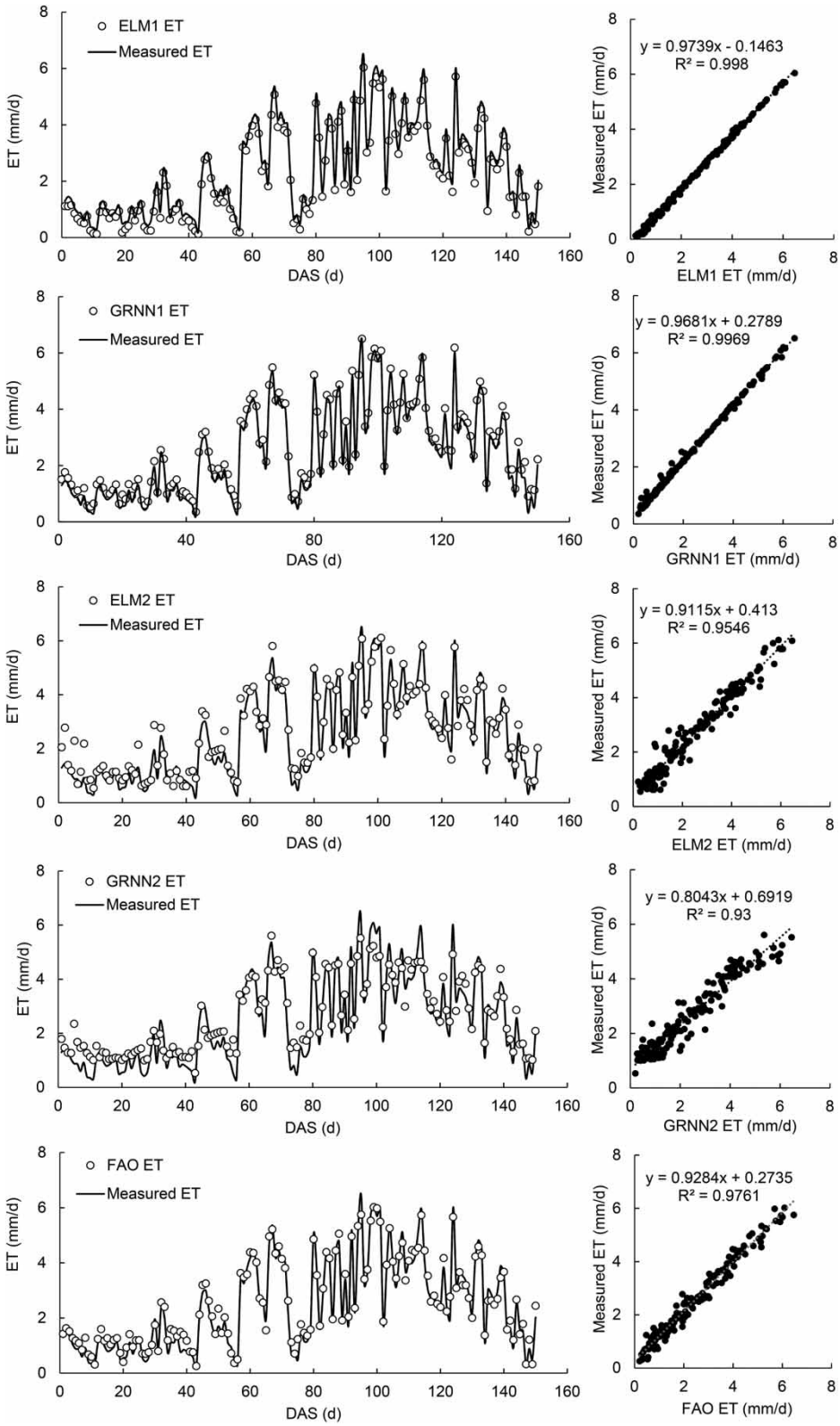

Figure 7 | Comparison of *ET* estimated by ELM, GRNN, and FAO-56 dual K_c models with the measured ones during maize growing seasons of 2013.

regression was 0.968, with R^2 of 0.997; the ELM2 and GRNN2 models, with only meteorological inputs, demonstrated poorer performances than ELM1 and GRNN1, with the slope of linear regression of 0.912 ($R^2 = 0.955$) and 0.804 ($R^2 = 0.93$), respectively, indicating *LAI* and h_c were very influential parameters for *ET* estimation. The modified dual K_c approach showed a slightly poorer performance than those of the ELM1 and GRNN1 models, with the slope of linear regression of 0.928 ($R^2 = 0.976$). Obvious underestimation of *ET* can be observed in the initial stage for the ELM1 model while GRNN1, ELM2, GRNN2, and dual K_c models overestimated *ET* in the initial stage. Compared with FAO-56 dual K_c approach, ELM1 and GRNN1 had higher goodness-of-fit, which confirmed the capabilities of ELM1 and GRNN1 for *ET* estimation.

Statistical performances of ELM, GRNN, and dual K_c models for maize *ET* estimation in 2013 are presented in Table 3. Based on the statistical indicators, ELM1 had the best performances for *ET* estimation, with RMSE of 0.221 mm/d, MAE of 0.203 mm/d, and NS of 0.981, respectively; estimated *ET* by ELM1 was 364.8 mm, which was 1.3% lower than measured *ET*. GRNN1 had good performances for *ET* estimation, too, with RMSE of 0.225 mm/d, MAE of 0.211 mm/d, and NS of 0.981, respectively; estimated *ET* by GRNN1 was 378.3 mm, which was 2.4% greater than measured *ET*. The performances of FAO-56 dual K_c approach were poorer than those of ELM1 and GRNN1, but better than those of ELM2 and GRNN2, with RMSE of 0.381 mm/d, MAE of 0.332 mm/d, and NS of 0.871, respectively. Although ELM2 and GRNN2 were not as efficient as ELM1, GRNN1, and dual K_c models, their estimation of *ET* was acceptable when only meteorological data were available.

Table 3 | Statistical performances of ELM, GRNN, and dual K_c models for maize *ET* estimation in 2013

Model	Estimated *ET* (mm)	Over/ Underestimation (%)	RMSE (mm/d)	MAE (mm/d)	NS
ELM1	364.8	−1.3	0.221	0.203	0.981
GRNN1	378.3	2.4	0.225	0.211	0.981
ELM2	398.6	7.9	0.403	0.353	0.848
GRNN2	400.8	8.5	0.521	0.421	0.836
FAO-56	385.6	4.4	0.381	0.332	0.871

Overall, this study found that the ELM and GRNN models can be applied successfully for maize *ET* estimation. Compared with GRNN, ELM was more efficient. In contrast to traditional FFNN, ELM randomly chooses hidden nodes and analytically determines the output weights, which may result in better performances of ELM. Although good performances of ELM and GRNN were found, they have no physical basis and belong to a class of data-driven black-box approaches (Tabari *et al.* 2012, 2013). In addition, they cannot partition *ET* separately into evaporation and transpiration.

CONCLUSION

The potential of ELM and GRNN for estimation of rainfed maize evapotranspiration was investigated on the China Loess Plateau in this study. A field experiment was conducted during maize growing seasons of 2011–2013 for continuous measurements of maize *ET* with eddy covariance systems, meteorological variables with automatic weather station, *LAI*, and h_c. These data were used to train the ELM and GRNN models consisting of two combinations of meteorological and crop parameters. The ELM1 and GRNN1 models whose inputs were meteorological and crop data performed better than the modified dual K_c model, which confirmed the capabilities of ELM and GRNN models for maize *ET* estimation. Although the ELM2 and GRNN2 models using only meteorological data were not as efficient as ELM1, GRNN1, and dual K_c models, their accuracy for maize *ET* estimation was acceptable, and could be considered as a tool to estimate maize *ET* when crop data are insufficient.

ACKNOWLEDGEMENTS

We are grateful for the research grants from the National Natural Science Foundation of China (No. 51179194), National Key Technologies R&D Program of China (No. 2015BAD24B01, No. 2012BAD09B01) and Basic Science Research Foundation of China Central Government (BSRF201609). Cordial thanks are extended to the editor and three anonymous reviewers for their valuable comments.

REFERENCES

Abdullah, S. S. A., Malek, M. A., Abdullah, N. S., Kisi, O. & Yap, K. S. 2015 Extreme learning machines: a new approach for prediction of reference evapotranspiration. *J. Hydrol.* **527**, 184–195.

Allen, R. G. 2000 Using the FAO-56 dual crop coefficient method over an irrigated region as part of an evapotranspiration intercomparison study. *J. Hydrol.* **229**, 27–41.

Allen, R. G. & Pereira, L. S. 2009 Estimating crop coefficients from fraction of ground cover and height. *Irrig. Sci.* **28** (1), 17–34.

Allen, R. G., Pereira, L. S., Raes, D. & Smith, M. 1998 *Crop evapotranspiration – Guidelines for computing crop water requirements*. FAO Irrigation and Drainage Paper No. 56. FAO, Rome, Italy.

Allen, R. G., Pereira, L. S., Howell, T. A. & Jensen, M. E. 2011 Evapotranspiration information reporting: I. Factors governing measurement accuracy. *Agric. Water Manage.* **98**, 899–920.

Brenner, A. J. & Incoll, L. D. 1997 The effect of clumping and stomatal response on evaporation from sparsely vegetated shrublands. *Agric. For. Meteorol.* **84**, 187–205.

Ding, R. S., Kang, S. Z., Zhang, Y. Q., Hao, X. M., Tong, L. & Du, T. S. 2013 Partitioning evapotranspiration into soil evaporation and transpiration using a modified dual crop coefficient model in irrigated maize field with ground-mulching. *Agric. Water Manage.* **127**, 85–96.

Feng, Y., Cui, N. B., Wei, X. P., Zhao, L. & Wang, J. Q. 2014 Temporal-spatial distribution characteristics and causes analysis of reference crop evapotranspiration in hilly area of central Sichuan. *Trans. Chin. Soc. Agric. Eng.* **30** (14), 78–86 (in Chinese).

Feng, Y., Cui, N. B., Zhao, L., Hu, X. T. & Gong, D. Z. 2016 Comparison of ELM, GANN, WNN and empirical models for estimating reference evapotranspiration in humid region of Southwest China. *J. Hydrol.* **536**, 376–383.

Ferreira, M. I., Silvestre, J., Conceicao, N. & Malheiro, A. C. 2012 Crop and stress coefficients in rainfed and deficit irrigation vineyards using sap flow techniques. *Irrig. Sci.* **30**, 433–447.

Gong, D. Z., Hao, W. P., Mei, X. R., Gao, X., Liu, Q. & Caylor, K. 2015 Warmer and wetter soil stimulates assimilation more than respiration in rainfed agricultural ecosystem on the China Loess Plateau: the role of partial plastic film mulching tillage. *PLoS One* **10** (8), e0136578.

Huang, G. B., Zhu, Q. Y. & Siew, C. K. 2006 Extreme learning machine: theory and applications. *Neurocomputing* **70** (1–3), 489–501.

Katerji, N. & Rana, G. 2006 Modelling evapotranspiration of six irrigated crops under Mediterranean climate conditions. *Agric. For. Meteorol.* **138**, 142–155.

Kim, S. & Kim, H. S. 2008 Neural networks and genetic algorithm approach for nonlinear evaporation and evapotranspiration modeling. *J. Hydrol.* **351**, 299–317.

Kisi, O. 2006 Generalized regression neural networks for evapotranspiration modeling. *Hydrol. Sci. J.* **51** (6), 1092–1105.

Kisi, O. 2008 The potential of different ANN techniques in evapotranspiration modelling. *Hydrol. Process.* **22**, 2449–2460.

Kisi, O. 2013 Applicability of Mamdani and Sugeno fuzzy genetic approaches for modeling reference evapotranspiration. *J. Hydrol.* **504**, 160–170.

Kisi, O. 2016 Modeling reference evapotranspiration using three different heuristic regression approaches. *Agric. Water Manage.* **169**, 162–172.

Kisi, O., Pour Ai Baba, A. & Shiri, J. 2012 Generalized neuro-fuzzy models for estimating daily pan evaporation values from weather data. *J. Irrig. Drain. Eng.* **138** (4), 1–14.

Kumar, M., Raghuwanshi, N. S., Singh, R., Wallender, W. W. & Pruitt, W. O. 2002 Estimating evapotranspiration using artificial neural network. *J. Irrig. Drain. Eng.* **128** (4), 224–233.

Ladlani, I., Houichi, L., Djemili, L., Heddam, S. & Belouz, K. 2012 Modeling daily reference evapotranspiration (ET_0) in the north of Algeria using generalized regression neural networks (GRNN) and radial basis function neural networks (RBFNN): a comparative study. *Meteorol. Atmos. Phys.* **118**, 163–178.

Landeras, G., Ortiz-Barredo, A. & Lopez, J. J. 2008 Comparison of artificial neural network models and empirical and semi-empirical equations for daily reference evapotranspiration estimation in the basque country (Northern Spain). *Agric. Water Manage.* **95**, 553–565.

Li, Z. Q., Yu, G. R., Wen, X. F., Zhang, L. M., Ren, C. Y. & Fu, Y. L. 2005 Energy balance closure at chinaFLUX sites. *Sci. China Earth Sci.* **48** (Suppl. 1), 51–62.

Li, S. E., Kang, S. Z., Li, F. S. & Zhang, L. 2008 Evapotranspiration and crop coefficient of spring maize with plastic mulch using eddy covariance in northwest China. *Agric. Water Manage.* **95** (11), 1214–1222.

Liu, Y. & Luo, Y. 2010 A consolidated evaluation of the FAO-56 dual crop coefficient approach using the lysimeter data in the North China Plain. *Agric. Water Manage.* **97**, 31–40.

Martí, P., Manzano, J. & Royuela, A. 2011a Assessment of a 4-input artificial neural network for ET_0 estimation through data set scanning procedures. *Irri. Sci.* **29** (3), 181–195.

Martí, P., González-Altozano, P. & Gasque, M. 2011b Reference evapotranspiration estimation without local climatic data. *Irrig. Sci.* **29** (6), 469–495.

Martí, P., González-Altozano, P., López-Urrea, R., Mancha, L. & Shiri, J. 2015 Modeling reference evapotranspiration with calculated targets: assessment and implications. *Agric. Water Manage.* **149** (2), 81–90.

Monteith, J. L. 1965 *Evaporation and Environment: 19th Symposia of the Society for Experimental Biology*. Cambridge University Press, Cambridge.

Mueller, N. D., Gerber, J. S., Johnston, M., Ray, D. K., Ramankutty, N. & Foley, J. A. 2012 Closing yield gaps through nutrient and water management. *Nature* **490** (7419), 254–257.

Newman, B. D., Archer, S. R., Breshears, D. D., Dahm, C. N., Duffy, C. J., McDowell, N. G., Phillips, F. M., Scanlon, B. R. & Vivoni, E. R. 2006 Ecohydrology of water-limited environments: a scientific vision. *Water Resour. Res.* **42** (6), W06302.

Poblete-Echeverría, C. A. & Ortega-Farias, S. O. 2013 Evaluation of single and dual crop coefficients over a drip-irrigated Merlot vineyard (Vitis vinifera L.) using combined measurements of sap flow system and an eddy covariance system. *Aust. J. Grape Wine Res.* **19**, 249–260.

Pour Ali Baba, A., Shiri, J., Kisi, O., FakheriFard, A., Kim, S. & Amini, A. 2013 Estimating daily reference evapotranspiration using available and estimated climatic data by adaptive neuro-fuzzy inference system (ANFIS) and artificial neural network (ANN). *Hydrol. Res.* **44** (1), 131–146.

Rana, G. & Katerji, N. 2000 Measurement and estimation of actual evapotranspiration in the field under Mediterranean climate: a review. *Eur. J. Agron.* **13**, 125–153.

Rasouli, K., Hsieh, W. W. & Cannon, A. J. 2012 Daily streamflow forecasting by machine learning methods with weather and climate inputs. *J. Hydrol.* **414**, 284–293.

Rousseaux, M. C., Figuerola, P. I., Correa-Tedesco, G. & Searles, P. S. 2009 Seasonal variations in sap flow and soil evaporation in an olive (Olea europaea L.) grove under two irrigation regimes in an arid region of Argentina. *Agric. Water Manage.* **96**, 1037–1044.

Shiri, J. & Kisi, O. 2011 Application of artificial intelligence to estimate daily pan evaporation using available and estimated climatic data in the Khozestan Province (Southwestern Iran). *J. Irrig. Drain. Eng.* **137** (7), 412–425.

Shiri, J., Kisi, O., Landeras, G., Lopez, J. J., Nazemi, A. H. & Stuyt, L. C. P. M. 2012 Daily reference evapotranspiration modeling by using genetic programming approach in the Basque Country (Northern Spain). *J. Hydrol.* **414**, 302–316.

Shiri, J., Nazemi, A. H., Sadraddini, A. A., Landeras, G., Kisi, O. & Marti, P. 2013 Global cross-station assessment of neuro-fuzzy models for estimating daily reference evapotranspiration. *J. Hydrol.* **480**, 46–57.

Shiri, J., Marti, P. & Singh, V. P. 2014a Evaluation of gene expression programming approaches for estimating daily pan evaporation through spatial and temporal data scanning. *Hydrol. Process.* **28** (3), 1215–1225.

Shiri, J., Sadraddini, A. A., Nazemi, A. H., Kisi, O., Landeras, G., Fard, A. F. & Martí, P. 2014b Generalizability of gene expression programming-based approaches for estimating daily reference evapotranspiration in coastal stations of Iran. *J. Hydrol.* **508**, 1–11.

Shiri, J., Nazemi, A. H., Sadraddini, A. A., Landeras, G., Kisi, O., Fard, A. F. & Marti, P. 2014c Comparison of heuristic and empirical approaches for estimating reference evapotranspiration from limited inputs in Iran. *Comput. Electron. Agr.* **108**, 230–241.

Shiri, J., Marti, P., Nazemi, A. H., Sadraddini, A. A., Kisi, O., Landeras, G. & Fakheri Fard, A. 2015 Local vs. external training of neuro-fuzzy and neural networks models for estimating reference evapotranspiration assessed through k-fold testing. *Hydrol. Res.* **46** (1), 72–88.

Shuttleworth, W. J. & Wallace, J. S. 1985 Evaporation from sparse crops – an energy combination theory. *Q. J. Roy. Meteor. Soc.* **111** (469), 839–855.

Specht, D. F. 1991 A general regression neural network. *IEEE T. Neural Netw.* **2** (6), 568–576.

Tabari, H., Kisi, O., Ezani, A. & Talaee, P. H. 2012 SVM, ANFIS, regression and climate based models for reference evapotranspiration modeling using limited climatic data in a semi-arid highland environment. *J. Hydrol.* **44**, 78–89.

Tabari, H., Martinez, C., Ezani, A. & Talaee, P. H. 2013 Applicability of support vector machines and adaptive neurofuzzy inference system for modeling potato crop evapotranspiration. *Irrig. Sci.* **31** (4), 575–588.

Taormina, R. & Chau, K. W. 2015 Data-driven input variable selection for rainfall-runoff modeling using binary-coded particle swarm optimization and extreme learning machines. *J. Hydrol.* **529**, 1617–1632.

Trajkovic, S., Todorovic, B. & Stankovic, M. 2003 Forecasting of reference evapotranspiration by artificial neural networks. *J. Irrig. Drain. Eng.* **129** (6), 454–457.

Traore, S., Wang, Y. M. & Kerh, T. 2010 Artificial neural network for modeling reference evapotranspiration complex process in Sudano-Sahelian zone. *Agric. Water Manage.* **97**, 707–714.

Wilson, K. B., Goldstein, A. H., Falge, E., Aubinet, M., Baldocchi, D. D., Berbigier, P., Bernhofer, C., Ceulemans, R., Dolman, H., Field, C., Grelle, A., Ibrom, A., Law, B. E., Kowalski, A., Meyers, T., Moncrieff, J., Monson, R., Oechel, W., Tenhunen, J., Valentini, R. & Verma, S. 2002 Energy balance closure at FLUXNET sites. *Agric. For. Meteorol.* **113**, 223–243.

Wolf, A., Saliendra, N., Akshalov, K., Johnson, D. A. & Laca, E. 2008 Effects of different eddy covariance correction schemes on energy balance closure and comparisons with the modified Bowen ratio system. *Agric. For. Meteorol.* **148**, 942–952.

Xu, C. Y. & Singh, V. P. 2005 Evaluation of three complementary relationship evapotranspiration models by water balance approach to estimate actual regional evapotranspiration in different climatic regions. *J. Hydrol.* **308**, 105–121.

Zhang, B. Z., Liu, Y., Xu, D., Zhao, N. N., Lei, B., Rosa, R. D., Paredes, P., Paco, T. A. & Pereira, L. S. 2013 The dual crop coefficient approach to estimate and partitioning evapotranspiration of the winter wheat-summer maize crop sequence in North China Plain. *Irrig. Sci.* **31** (6), 1303–1316.

Zhao, P., Li, S. E., Li, F. S., Du, T. S., Tong, L. & Kang, S. Z. 2015 Comparison of dual crop coefficient method and Shuttleworth-Wallace model in evapotranspiration partitioning in a vineyard of northwest China. *Agric. Water Manage.* **160**, 41–56.

First received 26 March 2016; accepted in revised form 13 July 2016. Available online 30 August 2016